INTERNATIONAL JOURNAL OF ADVANCED ENGINEERING AND BUSINESS SCIENCES (IJAEBS)

Journal homepage: https://ijaebs.journals.ekb.eg

# A Strut and Tie Model for Steel Fiber Reinforced Concrete Deep Beams

**F.B.A. Beshara[a], Ahmed. A. Mahmoud[*b] and A. A. El-Barbary[c]**

a Associate Professor, Department of civil engineering, faculty of engineering (Shoubra), Benha University,108 Shoubra St., Shoubra, Cairo, Egypt

b Professor of Reinforced Concrete Structures, Department of civil engineering, faculty of engineering (Shoubra), Benha University,108 Shoubra St., Shoubra, Cairo, Egypt

c Assistance Professor of Structural Engineering, Delta Higher Institute for Engineering and Technology, El Mansoura, Egypt

*Corresponding author: Email address: ahmed.m5882@gmail.comn

**Received**: 24-09-2022 **Accepted:** 19-11-2022 **Published**: 05-06-2023

## ABSTRACT

A modified Strut-and-Tie model (MSTM) was developed for fibrous deep beams to include the contribution of steel fibers in the internal resistance for compression and tension. The proposed (MSTM) calculates the ultimate loads for several experimental results. The ratio between experimental results and MSTM predictions ($P_{u(EXP)}/P_{u(MSTM)}$) for 79 specimens is 1.20%. The results of the Strut-and-Tie for the American Code ($P_{u(ACI)}$) and Egyptian Code ($P_{u(ECCS)}$) are more conservative. The inclusion of steel fibers increases the shear capacity of deep beams by 13% and 19% respectively in compassion with ACI Code and the Egyptian Code. The ratio for ($P_{u(EXP)}/P_{u(ACI)}$) and ($P_{uEXP}/P_{u(ECCS)}$) are 1.36 and 1.43, respectively. The predictions of (MSTM) are consistent, accurate, and have a great degree of validation for (HSSFRC) deep beams with different geometrical properties, concrete compressive strength, fibers, main and web steel ratios.

**Keywords:** Shear strength; High strength concrete; Deep beams; Steel fibers; Strut and Tie model.

# 1 INTRODUCTION

The Strut -and- Tie- Model can be used for the design of Disturbed regions (D-region) of structures where the basic assumption of flexure theory, namely plane sections remaining plane before and after bending, does not hold true. Such regions occur near statical discontinuities arising from concentrated forces or reactions and near geometric discontinuities, such as abrupt changes in cross section. The Strut -and- Tie- Model of design is based on the assumption that the D-regions in concrete structures can be analyzed and designed using hypothetical pin-jointed trusses consisting of struts and ties inter-connected at nodes.

In this paper, a number of modifications have been made to the strut-and- tie model (STM) presented in [1] for steel fibers RC deep beams. First, some assumptions and definitions are listed then, mathematical formulation of proposed STM is given to fully describe the geometry, derivation of internal forces, evaluation of compressive and tensile stresses, considerations of concrete tension softening, and to give a derivation for shear strength capacity. Second, procedure for design of RC steel fibers deep beams is given followed by worked design example. In addition, validation studies for the modified STM were made of eighty-five tested beams from the current research and other researchers from the literature. Finally, a comparative study for the results of proposed STM with the models given by the ECP 203-2018 [2] and the ACI code [3] is presented. The sensitivity of the proposed STM to design of steel fibers RC deep beams was checked lately by reliability study based on the available test results of the eighty-five specimens. In the reliability study, the effect of the shear span-to-depth ($a/d$) ratio, steel fiber volume ($V_f$) and steel fiber aspect ratio ($l_f/\phi_f$) on the experimental -versus- predicted strengths was illustrated.

# 2 MATHIMATICAL MODLING OF PROPOSED STM

## 2.1 Geometrical Discretization

The proposed STM model is similar to the STM model illustrated in American Code ACI Code 318-19 [3], and Egyptian Code ECP 203-2018 [2] with some modifications due to steel fibers inclusion which are listed as the following:

1) The top strut in the model is always prismatic, and the diagonal struts are tapered shape;
2) Improvement in compression strength of concrete is due to steel fiber inclusion;

3) Tensile resistance is represented by composite tie action due to steel reinforcement and steel fibers; and
4) The strut efficiency factor ($\beta_{sf}$) and nodal zone stress condition factor ($\beta_{nf}$) of fibrous concrete are instead of strut efficiency factor ($\beta_s$) and nodal zone stress condition factor ($\beta_n$) of normal concrete.

A STM for simply supported deep beams with two points load is given in Fig. 1. The deep beam under consideration can be assumed to be made up of a primary tension bottom tie, tow diagonal compression struts and one top compression. The angle between the axes of the struts and ties acting on a node should be as large as possible to mitigate cracking and to avoid incompatibilities due to shortening of the struts and lengthening of the tie occurring otherwise in almost the same directions. The location and orientation of the struts and tie is defined by the position of the nodes. The horizontal position of the nodes can be assumed to lie on the line of action of the respective applied loads and the support reactions. For vertical position of nodes, in order to exploit the full load carrying capacity of the beam, it is imperative that nodes A and D lie as close as possible to the bottom face of the beam. Similarly, the nodes B and C should lie as close as possible to the top face of the beam with providing sufficient concrete cover to the tie reinforcement. The assumed tie width will should be checked for adequacy with respect to the calculated tie force and the permissible stress in concrete in the node anchoring the tie. A STM for deep beams in plain or fibrous concrete with main steel and subjected to a vertical force, $V_u$=P/2, applied at distance ($a$) from the supported section, is schematically represented in Fig. 1. The deep beams had height ($h$) and base ($b$). Main bars with diameter ($\Phi$) have full area ($A_s$). As shown in Fig. 2, the STM is idealized as a statically determinate truss. It is consisted of four members as follows;

1- Top horizontal strut (BC) with compression force ($F_{u,BC}$);
2- Two diagonal tapered struts (AB), (CD) with compression forces ($F_{u,AB}$),($F_{u,CD}$);and
3- Bottom tie (AD) with tension force ($F_{u,AD}$).

The angle of inclination which is shown in Fig. 1of the diagonal member ($\theta$) is defined as:

$$\theta = tan^{-1}\left(\frac{h-c_1-c_2}{a}\right) \quad (1)$$

Where:

($h$) = the beam total depth.

($a$) = the shear span measured from center lines between the load and support bearing plates.

($c_1$) = the cover distance from the top steel bars to the top beam end.

($c_2$) = the cover distance from the bottom longitudinal steel bars to the beam soffit.

The angle (θ) should be not less than 25 º (degrees) according to ACI 318-19[3] or($\theta$) equal 26 º (degrees) according to ECP 203-2018 [2] Code. The term ($A_{str1}$) is assumed to be the cross-sectional area at the top strut (*BC*).The terms while ($A_{str2b}$), ($A_{str2t}$) are considered to be the cross-sectional area at the bottom and top ends of the tapered concrete strut (*AB*) and (*CD*). Finally ($A_{ct}$) is the cross-sectional area of the bottom tie (*AD*) as shown in Fig. 3 from the basic geometry relations, these terms are expressed by:

$$A_{str1} = b.\ w_s \quad (2)$$

$$A_{str2b} = b.\ w_{sb} = b.\ (w_{ct}\ cos\theta + l_b\ sin\theta) \quad (3)$$

$$A_{str2t} = b.\ w_{st} = b.\ (w_s\ cos\theta + l_b\ sin\theta) \quad (4)$$

$$A_{ct} = b.\ w_{ct} \quad (5)$$

Where:

($w_s$) is the width of the top strut.

($w_{st}$) is top end width of the tapered diagonal strut.

($w_{sb}$) is bottom end width of the tapered diagonal strut.

($w_{ct}$) is bottom composite tie width.

($l_b$) is the width of load or support bearing plate.

## 2.2 Strength of Compression Strut and Composite Tie

The compression capacity a strut ($F_c$) can be estimated depending on the shape of strut and it can be calculated generally as:

$$F_c = f_{cd}.\ A_{str} \quad (6)$$

Where: $A_{str}$ = cross-sectional area of the strut at the strut end under consideration.

$f_{cd}$ = effective compressive strength of fibrous concrete strut.

For prismatic strut, it is taken as ($f_{cd1}$)

$$f_{cd1} = z.\ \beta_{sf}.\ f_{cuf} \quad (7)$$

For tapered strut, it is taken as the smaller of ($f_{cd1}$) and ($f_{cd2}$). The value of ($f_{cd2}$) is the effective compressive strength of the fibrous concrete in the nodal zone.

$$f_{cd2} = z.\ \beta_{nf}.\ f_{cuf} \quad (8)$$

The coefficient (z) depends on the design code. It is taken as 0.67 for Egyptian Code ECP 203-2018 [2]. ($f_{cuf}$) is the compressive strength of the fibrous concrete. To include the gain in strength due to fibers inclusion, ($f_{cuf}$) is evaluated [4] by

$$f_{cuf} = f_{cu}\ (1+ 0.1066\ F\ ) \quad (9)$$

$$F = \frac{V_f\ l_f}{\phi_f} \quad (10)$$

Where ($F$) is the fiber factor, ($V_f$) is the fiber content ratio, ($l_f$) is the fiber length and ($\phi_f$) is the fiber diameter. The strut efficiency factor ($\beta_{sf}$) of fibrous concrete and the nodal zone efficiency factor of fibrous concrete ($\beta_{nf}$) are utilized [5] as:

$$\beta_{sf} = \beta_s + 0.28F \quad (11)$$

$$\beta_{nf} = \beta_n + 0.28\ F \quad (12)$$

Where ($\beta_s$) is the strut efficiency factor for non- fibrous concrete and it is determined according to shape of strut. ($\beta_n$) is the nodal zone stress efficiency factor for non- fibrous concrete and it is evaluated according to the stress condition at the nodal zone. The different values of factors ($\beta_s$), ($\beta_n$) are tabled in Table 1.

The compressive force in horizontal top strut ($F_{u,BC}$) and the compressive force in the diagonal struts ($F_{u,AB}$ and $F_{u,CD}$) are given by

$$F_{u,BC} = f_{cd1}\ .\ A_{str1} \quad (13)$$

$$F_{u,AB} = f_{cd2}\ .\ A_{str2b} \quad \text{(for nodal zone A)} \quad (14)$$

$$F_{u,AB} = f_{cd2}\ .\ A_{str2t} \quad \text{(for nodal zone B)} \quad (15)$$

To define the member in tension, an equivalent member is considered having steel area as embedded in a concrete member in tension. The proposed tie is composite of the strength of the reinforcing steel and a hypothetical prism of surrounding fibrous concrete concentric with the axis of the tensile force.

This composite tie is shown in Fig. 4 and indicated with the finer hatched area. The effective area of composite tie is given by

$$A_s^{eff} = n_s.\,(w_{ct})^2 \quad (16)$$

$$A_s^{eff} = n_s.\,(2.c_2 + \phi_b)^2 \quad (17)$$

($n_s$) is the number of main bottom bars adopted for tension steel. The tensile strength of a composite tie ($T_{ct}$) is taken as:

$$T_{ct} = f_y\,.\,A_s + \sigma_{pc}\,.\,(A_s^{eff} - A_s) \quad (18)$$

Where ($A_s$) is the reinforcing area of steel bars in tension composite tie, and it defined as:

$$A_s = n_s.\,A_{bar} \quad (19)$$

Where ; ($A_{bar}$) is the reinforcing area of one steel bar, ($f_y$) is the yielding stress of the steel bars and ($\sigma_{pc}$) is the post-cracking tensile fibrous concrete strength, which is defined as [6]:

$$\sigma_{pc} = 0.2475\,.\,F.\,(f_{cuf})^{2/3} \quad (20)$$

The tension force in the lower composite tie ($F_{u,AD}$) is given by

$$F_{u,AD} = f_y\,.\,A_s + \sigma_{pc}\,.\,(A_s^{eff} - A_s) \quad (21)$$

$$F_{u,AD} = n_s\,.\left[\left(f_y.A_{bar}\right) + \sigma_{pc}\,((w_{ct})^2 - A_{bar})\right] \quad (22)$$

Structural behavior of concrete flange continuous deep beams with carbon fiber reinforced polymer (CFRP) was studied by [7]., Zakaria et al. [8] studied enhancement the shear behavior of concrete beams reinforced with hybrid-wires bars by using steel fibers . Many current reaches [9– 13] studied the Strut and Tie Model (STM) using different modifications.

## 2.3 Derivation of Internal Forces

As shown in Fig.2, the truss should have the strut (BC) and tie (AD) are required to equilibrate the truss, these strut and tie form a force couple,

$$F_{u,AD} = F_{u,BC} \quad (23)$$

From the equilibrium of nodal zone (A) and (B), as shown in Fig. 3.

$F_{u,AD} = z.\beta_{nf} .f_{cuf} . b. w_{ct} .cot$ (24)

$F_{u,BC} = z.\beta_{nf} .f_{cuf} . b. w_s .cot$ (25)

Form equating Eq. (24) and Eq. (25), we get

$$w_s = \frac{\beta_{nf}}{\beta_{sf}} . w_{ct} \quad (26)$$

As shown in Fig. 2, the lever arm, (*jd*), of the force couple can be calculated as:

$jd = h - (w_s/2) - (w_{ct}/2)$ (27)

From Eq. (26), the lever arm, (*jd*), can be rewritten as:

$$jd = h - \frac{1}{2} w_{ct} . \left(\frac{\beta_{nf}}{\beta_{sf}} + 1\right) \quad (28)$$

There is another definition to calculate angle of inclination ($\theta$) as:

$\theta = tan^{-1}(jd / a)$ (29)

By taking moment about nodal zone (A) as shown Fig. 2, so

$V_u . a = F_{u,BC} . jd$ (30)

From Eqs. (2), (7) and (13), the compressive force in top strut is given by

$F_{u,BC} = z . \beta_{sf} . f_{cuf} . b. w_s$ (31)

Substituting Eq. (31), (26) and (28) into Eq. (30), we get

$$V_u . a = z . \beta_{sf} . f_{cuf} . b . \left(\frac{\beta_{nf}}{\beta_{sf}}\right) . w_{ct} . \left[h - \frac{w_{ct}}{2}\left(\frac{\beta_{nf}}{\beta_{sf}} + 1\right)\right] \quad (32)$$

The above equation is quadratic in ($w_{ct}$). Then by solving this equation to calculate the values of ($w_s$) and ($w_{ct}$), the internal forces in all truss members can be determined as

$F_{u,BC} = F_{u,AD} = V_u . a / jd$ (33)

$F_{u,AB} = F_{u,CD} = V_u / sin(\theta)$ (34)

After calculating the internal forces in all truss members, check of diagonal strut and nodal zone strengths must be done.

For Diagonal Strut (AB):

The allowable strength of the diagonal strut ($F_{allDS}$) is taken as:

$$F_{allDS} = z.\beta_{sf}.f_{cuf}.\ b.\ w_{SD} \quad (35)$$

Where ($w_{SD}$) is the smaller value of bottom and top diagonal strut widths ($w_{sb}$) *and* ($w_{st}$), respectively. Then the internal force in the diagonal strut $F_{u,ABC} < F_{allDS}$ , else modify ($w_s$) and ($w_{ct}$) by increasing their values and make new calculations up to satisfy the last condition.

For Nodal Zone (A):

According to Eq. (21), the effective area of composite tie is given by

$$A_s{}^{eff} = \frac{F_{u,AD} - f_y.A_s}{\sigma_{pc}} + A_s \quad (36)$$

From Eqs. (36), and Eq. (22), the required width ($w_{ct\ req}$) is given by

$$w_{ct\ req} = \left[\sqrt{\left(\frac{F_{u,AD} - f_y.A_s}{\sigma_{pc}}\right) + A_s}\right] / n_s \quad (37)$$

The value of ($w_{ct\ req}$) should be not exceed the last calculated value of ($w_s$), otherwise modify ($w_s$) *and* ($w_{ct}$) by increasing their values and make new calculations up to satisfy the last condition.

For Nodal Zone (B):

From equation (15) the required width ($w_{s\ req}$) of strut BC is given

$$w_{s\ req} = (F_{u,BC}) / (0.67.\beta_{sf}.f_{cuf}.\ b) \quad (38)$$

The value of ($w_{s\ req}$) should be not exceed the last calculated value of ($w_s$), else change values of ($w_s$) *and* ($w_{ct}$) by increasing their values and make new calculations up to satisfy the last condition. With reference to the truss structure, two nodal zones (A) and (B) are identified in the STM for simply supported deep beam as shown in Fig. 2. Nodal zone (A) at the support is (C-C-T) type, while nodal zone (B) is (C-C-C) type. The free body diagram which is shown in Fig. 3, the equilibrium conditions give the axial force ($T$) in the main steel and in the concrete strut ($C$) expressed, respectively, by

$$T = F_{u,AD} = \frac{V_u}{\tan\theta} \quad \text{(Force in the composite tie)} \quad (39)$$

$$C = F_{u,BC} = \frac{V_u}{\tan\theta} \quad \text{(Forec in the compressed top strut)} \quad (40)$$

By using equation (22) and substitute in equation (39)

$$V_{u(1)} = n_s \cdot \left[\left(f_y \times A_{bar}\right) + \sigma_{pc}\left((w_{ct})^2 - A_{bar}\right)\right] \tan\theta \quad (41)$$

While by using equation (22) and substitute in equation (40)

$$V_{u(2)} = [\,0.67.\beta_{sf}.f_{cuf}.\,b.\,w_s\,].\tan\theta \quad (42)$$

The definition of the shear carrying capacity ($V_u$) is defined as the smaller value of equation (41) or (42).

# 3 VERIFICATION STUDIES

## 3.1 Analysis and Design Flow Charts

In this section, there are two flow charts provided for computer implementation. The first flow chart based on iterative procedures to analyze and calculate the ultimate shear strength of SFRC deep beams as shown in Fig. 5. The second flow chart presented design procedures to get the amount of main longitudinal and web reinforcement for SFRC deep beams as shown in Fig. 6.

## 3.2 Validation Studies with Experimental Results

The computing procedures of modified (STM) for fibrous deep beams can be easily implemented by hand calculations or a spreadsheet as mentioned before. Seventy-nine fibrous RC deep beams reported by other researchers [14, 15, and 16-19] and current research have been evaluated by the proposed model. The details of the specimens and the predicted-versus-actual ultimate strength ratios are summarized in Table 2. The tested beams had an overall depth ranging from 260 to 600 mm. and an (*a/d*) ratio from 0.44 to 1.86. The bottom longitudinal main reinforcement ratios ranged from 0.79%, to 3.55%. The vertical and horizontal web reinforcement ratios ranged from zero to 0.56%, and from zero to 1.71%, respectively. The concrete cube strengths ranged from 23.6 MPa to 82.9 MPa. In Table 2, the obtained ultimate experimental strength ($P_{u(EXP)}$), the predicted strength ($P_{u(MSTM)}$ ) using the Modified Strut and Tie Model, the predicted strength ($P_{u(ACI)}$) due to ACI Code 318-19 [3] and ($P_{u(ECCS)}$) due to Egyptian Code ECP 203-2018 [2] are listed and their relationships are plotted in Figures 7, 8 and 9. It is important to know that the predicated strength using ACI-code and Egyptian-Code has not taken the effect of fibers inclusion in consideration. The modified (MSTM) for fibrous deep beams generally performs well in predicting the ultimate strengths. The overall average value of the ratio between the experimental strength to the predicted strength of the modified STM ($P_{u(EXP)} / P_{u(MSTM)}$ ) is of value

1.20 with a standard deviation as 0.08. The overall average value of the ratio between the experimental strength to the predicted strength ($P_{u(EXP)} / P_{u(ACI)}$) is of value 1.36, a standard deviation of 0.09. The overall average value of the ratio between the experimental strength to the predicted strength ($P_{u(EXP)} / P_{u(ECCS)}$) is of value 1.43, a standard deviation of 0.09. ACI Code and the Egyptian Code are more conservative than the modified STM. It can be concluded from the validation study that the inclusion of steel fibers increases the shear carrying capacity of deep beams by 13% and 19% respectively in compassion with ACI Code and the Egyptian Code.

### 3.3 Sensitivity Studies with Experimental Results

Sensitivity studies were performed for the experimental results of different strut-and-tie models. The ratios ($P_{u(EXP)} / P_{u(MSTM)}$), ($P_{u(Exp)} / P_{u(ACI)}$) and ($P_{u(EXP)} / P_{u(ECCS)}$) are plotted versus different properties. These properties are related to:

1- Geometry, such as ($a/d$) ratio

2- Fibers parameters, such as fiber volume content ($V_f$) and fiber aspect ratio ($l_f/\phi_f$).

3- Strengths of Materials, such as concrete strength ($f_{cu}$) and main steel yield stress ($f_y$).

4-Reinforcement parameters, such as main steel ratio ($\rho_s$), where:

$$\rho_s = \frac{A_s}{b.d} \times 100 \qquad (43)$$

The following important results are obtained from sensitivity studies:

a) The effect of ($a/d$) versus the ultimate strength due to the modified (MSTM) , ACI Code 318-19 code [3] and Egyptian Code ECP 203-2018 [2] are shown respectively in Fig. 10. The scatter is very low and uniform for the entire set of this variable. This shows that the predictions are consistent and accurate for fibrous RC deep beams with different geometrical properties. Finally, the comparison of model predictions with 79 test results is on the safe side and gives consistent predictions. The best predictions of the presented STM are obtained with shear span-to-depth ratio ($a/d$) ranged from 0.5 to 0.8.

b) The effect of steel fiber volume ratio ($V_f$) on the ultimate strength due to the modified STM, ACI Code 318-19 code [3] and Egyptian Code ECP 203-2018 [2], respectively are shown in Fig. 11. The effect of steel fiber aspect ratio ($l_f / \phi_f$) on the ultimate strength due to the modified STM, ACI Code 318-19 code [1] and Egyptian Code ECP 203-2018 [2], respectively are illustrated in Fig. 12. It is shown that the scatter is very low and uniform for the entire set of this variable. The comparison of model predictions with 79 test results is on the safe side and gives consistent predictions. The best predictions of the modified (MSTM) are obtained with steel fiber volume ratio at ($V_f$) =1.0, the best predictions of the modified (MSTM) are obtained with steel fiber aspect ratio at ($l_f / \phi_f$) =100.

c) In Fig. 13, the effect of concrete compressive strength ($f_{cu}$) versus the ultimate strength due to the modified (MSTM), ACI Code 318-19 code [3] and Egyptian Code ECP 203-2018 [2], respectively is shown. The effect of steel yield stress ($f_y$) versus the ultimate strength due to the modified STM, ACI Code 318-19 code [3] and Egyptian Code ECP 203-2018 [2], respectively is illustrated in Fig. 14. It is shown that the scatter is very low and uniform for the entire set of this variable. The comparison of model predictions with 79 test results is on the safe side and gives consistent predictions. The best predictions of the modified (MSTM) are obtained with concrete compressive strength ($f_{cu}$) ranged from 50 to 66 N/mm$^2$ for high strength concrete, while the best predictions of the modified STM are obtained with steel yield stress ($f_y$) ranged from 360 to 460 N/mm$^2$.

d) The effect of main steel ratio ($\rho_s$) versus the ultimate strength due to the modified STM, ACI Code 318-19 code [3] and Egyptian Code ECP 203-2018 [2], respectively are shown in Fig. 15. The best predictions of the presented STM are obtained with main steel ratio ($\rho_s$) ranged from 0.68% to 1.0%. This shows that the predictions are consistent and accurate for fibrous RC deep beams with different fibers parameters.

# 4 CONCLUSION

From the analytical studies in the present work, some prominent conclusions can be drawn:

1. The Modified Strut-and-Tie Model (MSTM) accounts for the contribution of steel fibers in resisting tension and compression forces and so, it calculates the ultimate loads accurately and performs compatibly to the experimental results of provided 79 specimens, which show a satisfied performance. The overall average value of the ratio between the experimental strength to the predicted strength using MSTM ($P_{u(EXP)}/P_{u(MSTM))}$) is 1.21, with a standard deviation of 0.08.
2. The comparison between the testing results and analytical results of Strut-and Tie Model (STM) of American Code (ACI) and Egyptian Code (ECP) indicate that the available codes are more conservative than the (MSTM). It can be concluded from the validation study that the inclusion of steel fibers increases the shear carrying capacity of deep beams by 13% and 19% respectively in comparison with American Code and the Egyptian Code. The overall average value of ($P_{u(EXP)}/P_{u(ACI)}$) and ($P_{u(EXP)}/P_{u\ (ECP)}$) are (1.36 and 1.43%), with overall standard deviation of (0.09 and 0.09), respectively.
3. The reliability study of the (MSTM) indicates that the predictions are consistent, accurate, and have a great degree of validation for (HSSFRC) deep beams. The best predictions of (MSTM) are obtained with shear span-to-depth ratio ($a/d$) ranged from 0.5 to 0.8, with steel fiber volume ratio at ($V_f$) =1.0, with steel fiber aspect ratio at ($l_f/\phi_f$) =100, with concrete compressive strength ($f_{cu}$) ranged from 50 to 66 N/mm$^2$, with steel yield stress ($f_y$) ranged from 360 to 460 N/mm$^2$, and with main steel ratio ($\rho_s$) ranged from 0.68% to 1.0%.

**Table 1 Values of coefficient ($\beta_s$) and ($\beta_n$) used in the modified STM**

| Factor | Egyptian Code ECP 203-2018 | America Code ACI 318-19 Code |
|---|---|---|
| Strut efficiency factor ($\beta_s$) | | |
| a) Uniform cross-sectional area over its length (prismatic strut) | 1.00 | 1.00 |
| b) Bottle-shaped struts with web reinforcement | 0.70 | 0.75 |
| c) Nodal zone efficiency factor ($\beta_n$) | | |
| C-C-T nodal zones anchoring only one tie | 0.80 | 0.80 |

**Table 2** Predictions of Ultimate Loads

| *No.* | *Ref.* | $f_{cu}$ *(MPa)* | $f_y$ *(MPa)* | $\rho_s$ *(%)* | *a/d* | $V_f$ *%* | $l_f$ */$\phi_f$ | $P_{uExp}$ *(kN)* | $P_{uMSTM}$ *(kN)* | $P_{uSTM}$ *ACI (kN)* | $P_{uSTM}$ *ESSC (kN)* | $\frac{P_{uExp}}{P_{uMSTM}}$ | $\frac{P_{uExp}}{P_{uSTM}}$ *(ACI)* | $\frac{P_{uExp}}{P_{uSTM}}$ *(ESSC)* |
|---|---|---|---|---|---|---|---|---|---|---|---|---|---|---|
| 1 | [15] | 60.00 | 438 | 0.94 | 0.44 | 0.00 | 0 | 1150.0 | 953.0 | 833.3 | 803.2 | 1.21 | 1.38 | 1.43 |
| 2 | [15] | 63.50 | 438 | 0.94 | 0.44 | 0.50 | 80 | 1350.0 | 1024.3 | 912.2 | 863.3 | 1.32 | 1.48 | 1.56 |
| 3 | [15] | 64.00 | 438 | 0.94 | 0.44 | 1.00 | 60 | 1380.0 | 1078.9 | 954.8 | 909.3 | 1.28 | 1.45 | 1.52 |
| 4 | [15] | 65.00 | 438 | 0.94 | 0.44 | 1.00 | 80 | 1420.0 | 1234.4 | 1014.0 | 965.7 | 1.15 | 1.40 | 1.47 |
| 5 | [15] | 60.00 | 438 | 0.94 | 0.81 | 0.00 | 0 | 670.00 | 555.8 | 491.8 | 468.4 | 1.21 | 1.36 | 1.43 |
| 6 | [15] | 63.50 | 438 | 0.94 | 0.81 | 0.50 | 80 | 703.00 | 558.5 | 494.2 | 470.7 | 1.26 | 1.42 | 1.49 |
| 7 | [15] | 64.00 | 438 | 0.94 | 0.81 | 1.00 | 60 | 740.50 | 603.0 | 533.7 | 508.3 | 1.23 | 1.39 | 1.46 |
| 8 | [15] | 65.00 | 438 | 0.94 | 0.81 | 1.00 | 80 | 781.00 | 639.0 | 565.5 | 538.6 | 1.22 | 1.38 | 1.45 |
| 9 | [15] | 60.00 | 438 | 0.94 | 1.00 | 0.00 | 0 | 490.00 | 453.3 | 401.1 | 382.0 | 1.08 | 1.22 | 1.28 |
| 10 | [15] | 63.50 | 438 | 0.94 | 1.00 | 0.50 | 80 | 550.00 | 463.1 | 409.8 | 390.3 | 1.19 | 1.34 | 1.41 |
| 11 | [15] | 65.00 | 438 | 0.94 | 1.00 | 1.00 | 80 | 600.00 | 473.2 | 418.8 | 398.8 | 1.27 | 1.43 | 1.50 |
| 12 | [15] | 62.00 | 438 | 0.94 | 0.81 | 0.50 | 80 | 705.00 | 558.9 | 494.6 | 471.0 | 1.26 | 1.43 | 1.50 |
| 13 | [15] | 62.00 | 438 | 0.94 | 0.81 | 1.00 | 80 | 765.00 | 632.5 | 559.8 | 533.1 | 1.21 | 1.37 | 1.43 |
| 14 | [15] | 70.00 | 438 | 0.94 | 0.81 | 1.00 | 80 | 751.00 | 640.7 | 567.0 | 540.0 | 1.17 | 1.32 | 1.39 |
| 15 | [15] | 62.00 | 438 | 0.94 | 0.81 | 0.50 | 80 | 710.00 | 557.5 | 493.4 | 469.9 | 1.27 | 1.44 | 1.51 |
| 16 | [15] | 64.00 | 438 | 0.94 | 0.81 | 1.00 | 80 | 745.00 | 621.3 | 549.8 | 523.7 | 1.20 | 1.35 | 1.42 |
| 17 | [15] | 66.00 | 438 | 0.94 | 0.81 | 1.00 | 80 | 760.00 | 647.4 | 572.9 | 545.6 | 1.17 | 1.33 | 1.39 |
| 18 | [4] | 53.90 | 550 | 3.55 | 0.70 | 0.00 | 0 | 632.00 | 518.0 | 458.4 | 436.6 | 1.22 | 1.38 | 1.45 |

**Table 2** Predictions of Ultimate Loads (cont.)

| *No.* | *Ref.* | $f_{cu}$ *(MPa)* | $f_y$ *(MPa)* | $\rho_s$ *(%)* | *a/d* | $V_f$% | $l_f/\phi_f$ | $P_{uExp}$ *(kN)* | $P_{uMST}$ *(kN)* | $P_{uSTM}$ *ACI (kN)* | $P_{uSTM}$ *ESSC (kN)* | $\frac{P_{uExp}}{P_{uMSTM}}$ | $\frac{P_{uExp}}{P_{uSTM}}$ *(ACI)* | $\frac{P_{uExp}}{P_{uSTM}}$ *(ESSC)* |
|---|---|---|---|---|---|---|---|---|---|---|---|---|---|---|
| 19 | [4] | 64.50 | 550 | 3.55 | 0.70 | 0.25 | 100 | 700 | 593.2 | 525.0 | 500.0 | 1.18 | 1.33 | 1.40 |
| 20 | [4] | 62.20 | 550 | 3.55 | 0.70 | 0.50 | 100 | 650 | 565.2 | 500.2 | 476.4 | 1.15 | 1.30 | 1.36 |
| 21 | [4] | 58.00 | 550 | 3.55 | 0.70 | 0.75 | 100 | 722 | 633.3 | 560.5 | 533.8 | 1.14 | 1.29 | 1.35 |
| 22 | [4] | 68.20 | 550 | 3.55 | 0.70 | 1.00 | 100 | 792 | 707.1 | 625.8 | 596.0 | 1.12 | 1.27 | 1.33 |
| 23 | [4] | 67.00 | 550 | 3.55 | 0.70 | 1.25 | 100 | 786 | 714.5 | 632.3 | 602.2 | 1.10 | 1.24 | 1.31 |
| 24 | [4] | 61.60 | 550 | 3.55 | 0.46 | 1.00 | 100 | 908 | 776.1 | 686.8 | 654.1 | 1.17 | 1.32 | 1.39 |
| 25 | [4] | 58.30 | 550 | 3.55 | 0.58 | 1.00 | 100 | 808.00 | 696.6 | 616.4 | 587.1 | 1.16 | 1.31 | 1.38 |
| 26 | [4] | 55.60 | 550 | 3.55 | 0.81 | 1.00 | 100 | 684.00 | 594.8 | 526.4 | 501.3 | 1.15 | 1.30 | 1.36 |
| 27 | [4] | 59.90 | 550 | 3.55 | 0.93 | 1.00 | 100 | 688.00 | 608.8 | 538.8 | 513.1 | 1.13 | 1.28 | 1.34 |
| 28 | [4] | 37.80 | 550 | 3.55 | 0.70 | 1.00 | 100 | 588.00 | 509.5 | 450.9 | 429.4 | 1.15 | 1.30 | 1.37 |
| 29 | [4] | 42.30 | 550 | 3.55 | 0.70 | 1.00 | 100 | 666.00 | 584.2 | 517.0 | 492.4 | 1.14 | 1.29 | 1.35 |
| 30 | [16] | 28.56 | 440 | 1.94 | 0.32 | 1.00 | 60 | 750.00 | 572.5 | 506 .7 | 482.5 | 1.31 | 1.48 | 1.55 |
| 31 | [16] | 28.56 | 440 | 1.94 | 0.62 | 1.00 | 60 | 720.00 | 562.5 | 497.8 | 474.1 | 1.28 | 1.45 | 1.52 |
| 32 | [16] | 28.40 | 440 | 1.94 | 0.93 | 1.00 | 60 | 582.00 | 451.2 | 399.3 | 380.2 | 1.29 | 1.46 | 1.53 |
| 33 | [16] | 24.88 | 440 | 1.94 | 1.24 | 1.00 | 60 | 456.00 | 396.5 | 350.9 | 334.2 | 1.15 | 1.30 | 1.36 |
| 34 | [16] | 25.20 | 440 | 1.94 | 1.86 | 1.00 | 60 | 366.00 | 345.3 | 305.6 | 291.0 | 1.06 | 1.20 | 1.26 |
| 35 | [16] | 27.52 | 440 | 1.94 | 1.24 | 0.00 | 0 | 410.00 | 317.8 | 281.3 | 267.9 | 1.29 | 1.46 | 1.53 |
| 36 | [16] | 27.04 | 440 | 1.94 | 1.24 | 0.50 | 60 | 440.00 | 360.7 | 319.2 | 304.0 | 1.22 | 1.38 | 1.45 |
| 37 | [16] | 26.56 | 440 | 1.94 | 1.24 | 1.50 | 60 | 520.00 | 460.2 | 407.2 | 387.8 | 1.13 | 1.28 | 1.34 |

**Table 2** Predictions of Ultimate Loads (cont.).

| No. | Ref. | fcu (MPa) | fy (MPa) | □s (%) | a/d | Vf % | $l_f/\phi_f$ | $P_{uExp}$ (kN) | $P_{uMSTM}$ (kN) | $P_{uSTM}$ ACI (kN) | $P_{uSTM}$ ESSC (kN) | $\frac{P_{uExp}}{P_{uMSTM}}$ | $\frac{P_{uExp}}{P_{uSTM}}$ (ACI) | $\frac{P_{uExp}}{P_{uSTM}}$ (ESSC) |
|---|---|---|---|---|---|---|---|---|---|---|---|---|---|---|
| 38 | [16] | 23.60 | 440 | 1.94 | 1.52 | 1.00 | 60 | 448.00 | 407.3 | 360.4 | 343.3 | 1.10 | 1.24 | 1.31 |
| 39 | [16] | 24.08 | 440 | 1.94 | 1.52 | 1.00 | 60 | 580.00 | 532.1 | 470.9 | 448.5 | 1.09 | 1.23 | 1.29 |
| 40 | [17] | 85.40 | 403 | 3.64 | 0.79 | 0.50 | 32 | 610.00 | 495.9 | 438.9 | 418.0 | 1.23 | 1.39 | 1.46 |
| 41 | [17] | 89.30 | 403 | 3.64 | 0.79 | 1.00 | 32 | 645.00 | 551.3 | 487.9 | 464.6 | 1.17 | 1.32 | 1.39 |
| 42 | [17] | 93.70 | 403 | 3.64 | 0.79 | 2.00 | 32 | 690.00 | 621.6 | 550.1 | 523.9 | 1.11 | 1.25 | 1.32 |
| 43 | [17] | 85.40 | 403 | 3.64 | 0.79 | 0.50 | 32 | 534.00 | 423.8 | 375.1 | 357.2 | 1.26 | 1.42 | 1.49 |
| 44 | [17] | 89.30 | 403 | 3.64 | 0.79 | 1.00 | 32 | 586.00 | 492.4 | 435.8 | 415.0 | 1.19 | 1.34 | 1.41 |
| 45 | [17] | 93.70 | 403 | 3.64 | 0.79 | 2.00 | 32 | 615.00 | 580.2 | 513.4 | 489.0 | 1.06 | 1.20 | 1.26 |
| 46 | [17] | 85.40 | 403 | 3.64 | 0.94 | 0.50 | 32 | 523.00 | 428.7 | 379.4 | 361.3 | 1.22 | 1.38 | 1.45 |

| | | | | | | | | | | | | | | |
|---|---|---|---|---|---|---|---|---|---|---|---|---|---|---|
| 47 | [17] | 89.30 | 403 | 3.64 | 0.94 | 1.00 | 32 | 550.00 | 470.1 | 416.0 | 396.2 | 1.17 | 1.32 | 1.39 |
| 48 | [17] | 85.40 | 403 | 3.64 | 0.94 | 0.50 | 32 | 485.00 | 394.3 | 348.9 | 332.3 | 1.23 | 1.39 | 1.46 |
| 49 | [18] | 89.30 | 403 | 3.64 | 0.94 | 1.00 | 32 | 510.00 | 439.7 | 389.1 | 370.5 | 1.16 | 1.31 | 1.38 |
| 50 | [18] | 28.90 | 410 | 0.79 | 0.75 | 0.00 | 0 | 158.00 | 123.4 | 109.2 | 104.0 | 1.28 | 1.45 | 1.52 |
| 51 | [18] | 28.90 | 410 | 0.79 | 0.75 | 0.00 | 0 | 173.00 | 138.4 | 122.5 | 116.6 | 1.25 | 1.41 | 1.48 |
| 52 | [18] | 32.10 | 410 | 0.79 | 0.75 | 1.00 | 90 | 181.00 | 150.8 | 133.5 | 127.1 | 1.20 | 1.36 | 1.42 |
| 53 | [18] | 33.50 | 410 | 0.79 | 0.75 | 1.25 | 90 | 188.00 | 162.1 | 143.4 | 136.6 | 1.16 | 1.31 | 1.38 |
| 54 | [18] | 28.90 | 410 | 0.79 | 0.75 | 0.00 | 0 | 183.00 | 138.6 | 122.7 | 116.8 | 1.32 | 1.49 | 1.57 |
| 55 | [18] | 28.90 | 410 | 0.79 | 0.75 | 0.00 | 0 | 173.00 | 133.1 | 117.8 | 112.2 | 1.30 | 1.47 | 1.54 |
| 56 | [18] | 28.90 | 410 | 0.79 | 1.00 | 0.00 | 0 | 143.00 | 109.2 | 96.6 | 92.0 | 1.31 | 1.48 | 1.55 |

**Table 2** Predictions of Ultimate Loads (cont.)

| No. | Ref. | fcu (MPa) | fy MPa) | □s (%) | a/d | Vf % | $l_f/\phi_f$ | $P_{uExp}$ (kN) | $P_{uMSTM}$ (kN) | $P_{uSTM}$ ACI (kN) | $P_{uSTM}$ ESSC (kN) | $\frac{P_{uExp}}{P_{uMSTM}}$ | $\frac{P_{uExp}}{P_{uSTM}}$ (ACI) | $\frac{P_{uExp}}{P_{uSTM}}$ (ESSC) |
|---|---|---|---|---|---|---|---|---|---|---|---|---|---|---|
| 57 | [18] | 28.90 | 410 | 0.79 | 1.00 | 0.00 | 0 | 148.00 | 114.7 | 101.5 | 96.7 | 1.29 | 1.46 | 1.53 |
| 58 | [18] | 32.10 | 410 | 0.79 | 1.00 | 1.00 | 90 | 168.00 | 144.8 | 128.2 | 122.1 | 1.16 | 1.31 | 1.38 |
| 59 | [18] | 33.50 | 410 | 0.79 | 1.00 | 1.25 | 90 | 173.00 | 155.9 | 137.9 | 131.4 | 1.11 | 1.25 | 1.32 |
| 60 | [18] | 28.90 | 410 | 0.79 | 1.00 | 0.00 | 0 | 169.00 | 125.2 | 110.8 | 105.5 | 1.35 | 1.53 | 1.60 |
| 61 | [18] | 28.90 | 410 | 0.79 | 1.00 | 0.00 | 0 | 159.50 | 119.0 | 105.3 | 100.3 | 1.34 | 1.51 | 1.59 |
| 62 | [18] | 28.90 | 410 | 0.79 | 1.25 | 0.00 | 0 | 123.00 | 92.5 | 81.8 | 77.9 | 1.33 | 1.50 | 1.58 |
| 63 | [18] | 28.90 | 410 | 0.79 | 1.25 | 0.00 | 0 | 128.00 | 97.7 | 86.5 | 82.4 | 1.31 | 1.48 | 1.55 |
| 64 | [18] | 32.10 | 410 | 0.79 | 1.25 | 1.00 | 90 | 156.60 | 135.0 | 119.5 | 113.8 | 1.16 | 1.31 | 1.38 |
| 65 | [18] | 33.50 | 410 | 0.79 | 1.25 | 1.25 | 90 | 161.00 | 145.0 | 128.4 | 122.2 | 1.11 | 1.25 | 1.32 |
| 66 | [18] | 28.90 | 410 | 0.79 | 1.25 | 0.00 | 0 | 145.25 | 108.4 | 95.9 | 91.4 | 1.34 | 1.51 | 1.59 |
| 67 | [18] | 28.90 | 410 | 0.79 | 1.25 | 0.00 | 0 | 142.00 | 110.1 | 97.4 | 92.8 | 1.29 | 1.46 | 1.53 |
| 68 | [19] | 35.00 | 415 | 1.88 | 1.33 | 1.00 | 100 | 75.50 | 57.6 | 51.0 | 48.6 | 1.31 | 1.48 | 1.55 |
| 69 | [19] | 36.40 | 415 | 1.88 | 1.33 | 1.00 | 100 | 80.00 | 62.0 | 54.9 | 52.3 | 1.29 | 1.46 | 1.53 |
| 70 | [19] | 31.00 | 415 | 1.88 | 1.33 | 1.00 | 100 | 70.50 | 52.6 | 46.6 | 44.3 | 1.34 | 1.51 | 1.59 |
| 71 | [19] | 35.20 | 415 | 1.41 | 1.00 | 1.00 | 100 | 130.00 | 103.2 | 91.3 | 87.0 | 1.26 | 1.42 | 1.49 |
| 72 | [19] | 38.00 | 415 | 1.41 | 1.00 | 1.00 | 100 | 140.00 | 112.9 | 99.9 | 95.2 | 1.24 | 1.40 | 1.47 |
| 73 | [19] | 36.70 | 415 | 1.41 | 1.00 | 1.00 | 100 | 134.50 | 110.2 | 97.6 | 92.9 | 1.22 | 1.38 | 1.45 |
| 74 | [19] | 33.70 | 415 | 1.13 | 0.80 | 1.00 | 100 | 170.00 | 153.2 | 135.5 | 129.1 | 1.11 | 1.25 | 1.32 |
| 75 | [19] | 37.40 | 415 | 1.13 | 0.80 | 1.00 | 100 | 172.50 | 158.3 | 140.1 | 133.4 | 1.09 | 1.23 | 1.29 |

**Table 2** Predictions of Ultimate Loads (cont.)

| No. | Ref. | fcu (MPa) | fy (MPa) | □s (%) | a/d | Vf % | $l_f/\phi_f$ | $P_{uExp}$ (kN) | $P_{uMSTM}$ (kN) | $P_{uSTM}$ ACI (kN) | $P_{uSTM}$ ESSC (kN) | $P_{uExp}$ / $P_{uMSTM}$ | $P_{uExp}$ / $P_{uSTM}$ (ACI) | $P_{uExp}$ / $P_{uSTM}$ (ESSC) |
|---|---|---|---|---|---|---|---|---|---|---|---|---|---|---|
| 76 | [19] | 38.60 | 415 | 1.13 | 0.80 | 1.00 | 100 | 178.50 | 168.4 | 149.0 | 141.9 | 1.06 | 1.20 | 1.26 |
| 77 | [19] | 34.50 | 415 | 0.92 | 0.67 | 1.00 | 100 | 236.00 | 210.7 | 186.5 | 177.6 | 1.12 | 1.27 | 1.33 |
| 78 | [19] | 35.20 | 415 | 0.92 | 0.67 | 1.00 | 100 | 237.00 | 213.5 | 188.1 | 182.3 | 1.11 | 1.26 | 1.30 |
| 79 | [19] | 31.30 | 415 | 0.92 | 0.67 | 1.00 | 100 | 226.50 | 204.1 | 180.6 | 172.0 | 1.11 | 1.25 | 1.32 |
| | | | | | | | | Average | | | | 1.20 | 1.36 | 1.43 |
| | | | | | | | | Standard Deviation (SD) | | | | 0.08 | 0.09 | 0.09 |

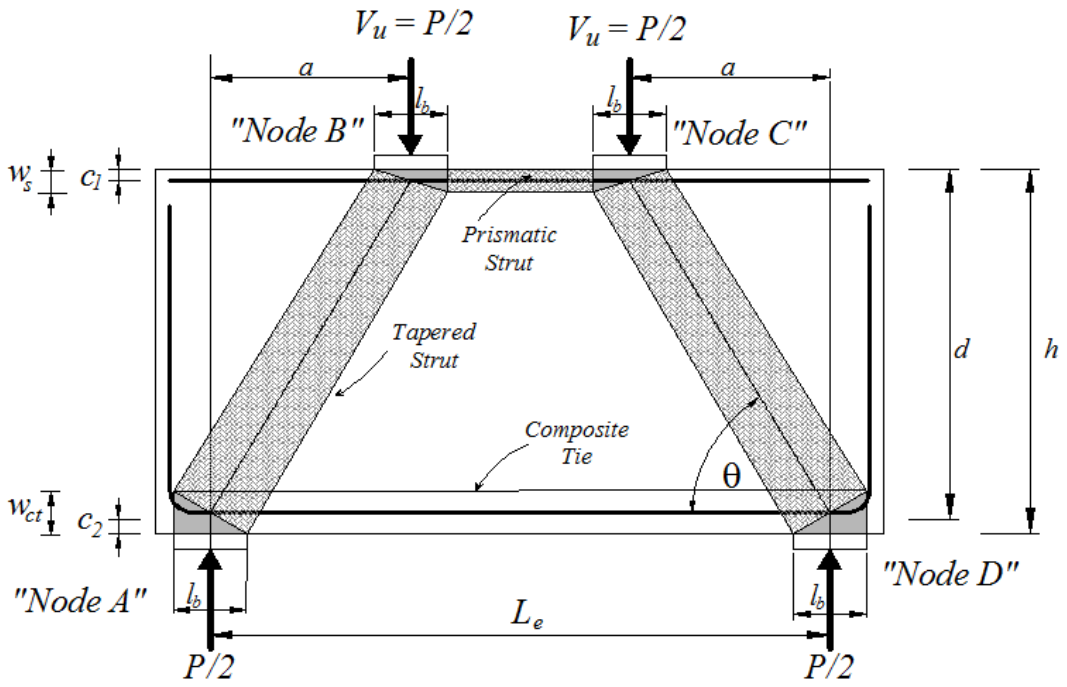


**Fig. 1. Strut and Tie Model of HSFRCD Deep Beam.**

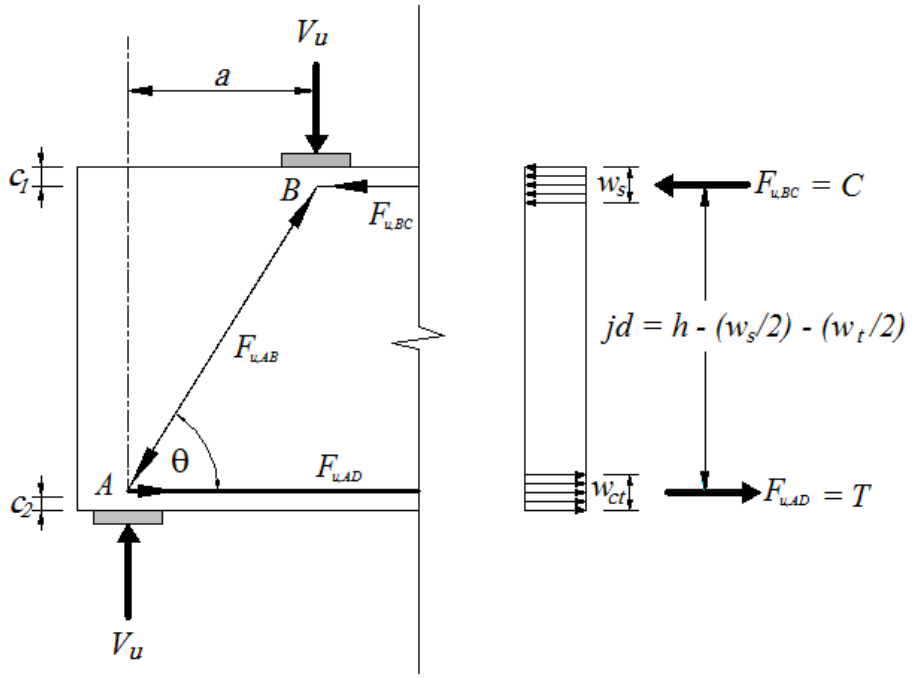


**Fig. 2. Truss Model for Modified STM of HSFRC Deep Beams.**

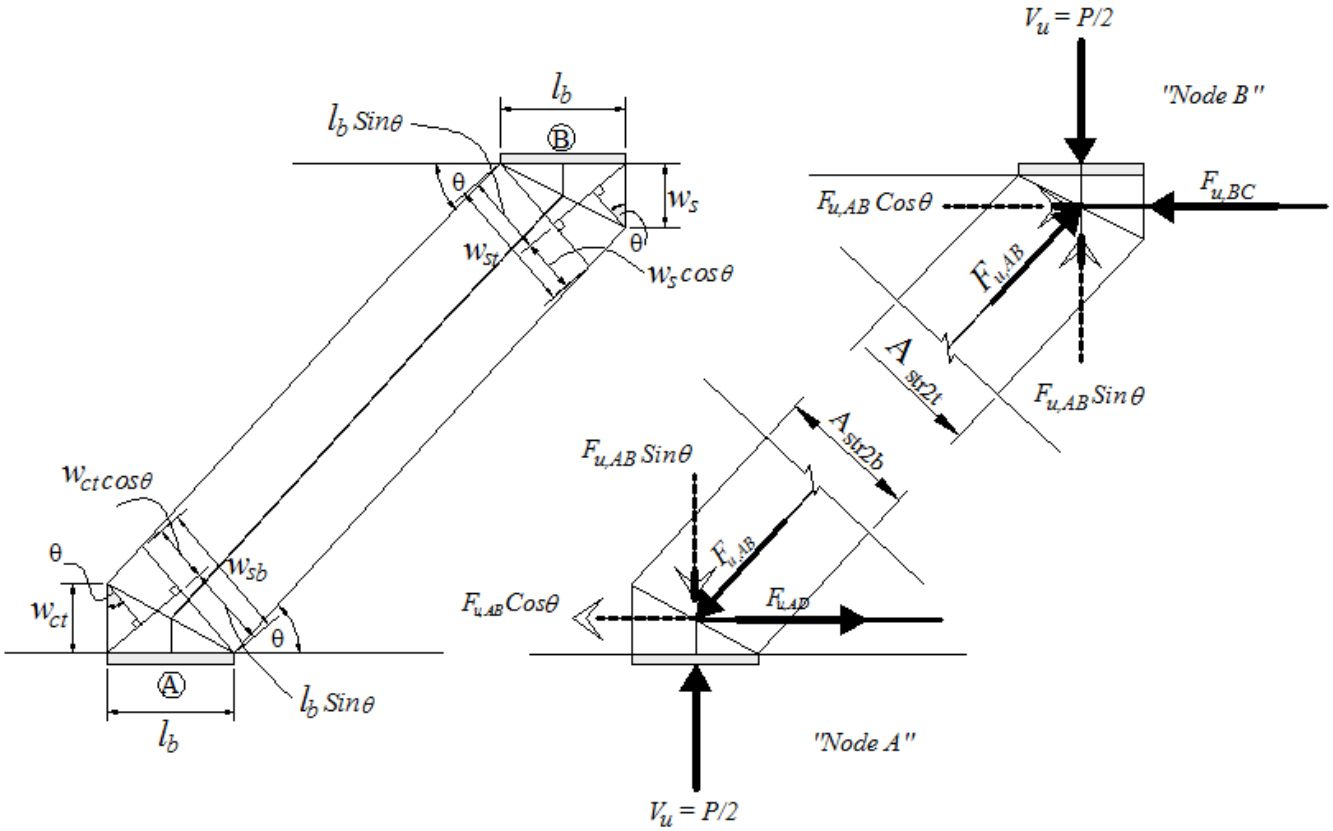


**Fig. 3. Geometric Details of Nodal Zones (A & B) of Tapered Strut and Their Forces.**

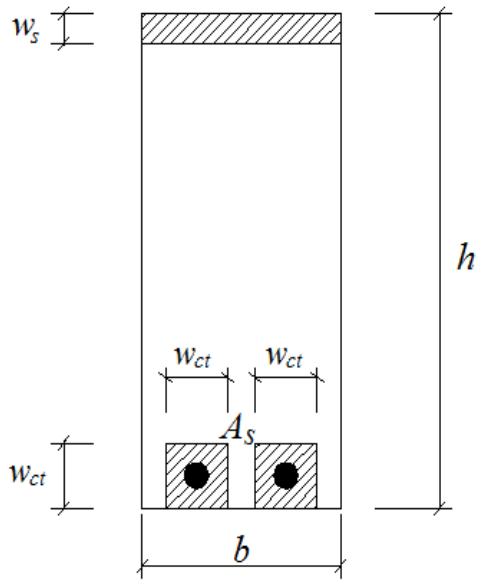


**Fig. 4. Details of the Composite Tie of Fibrous Concrete.**

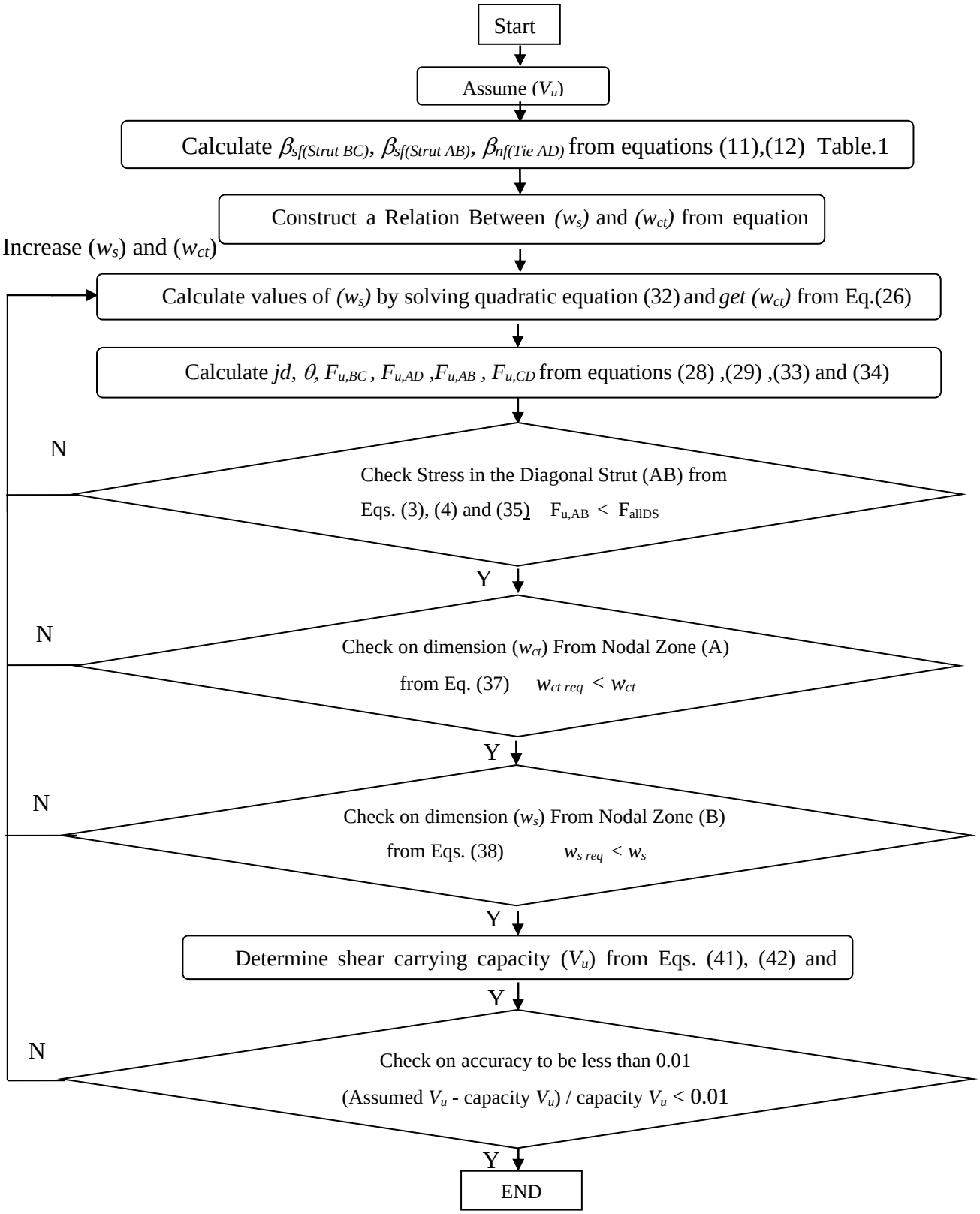


Fig. 5. Iterative Procedure for Computing the Ultimate Strength of HSFRC Deep Beams.

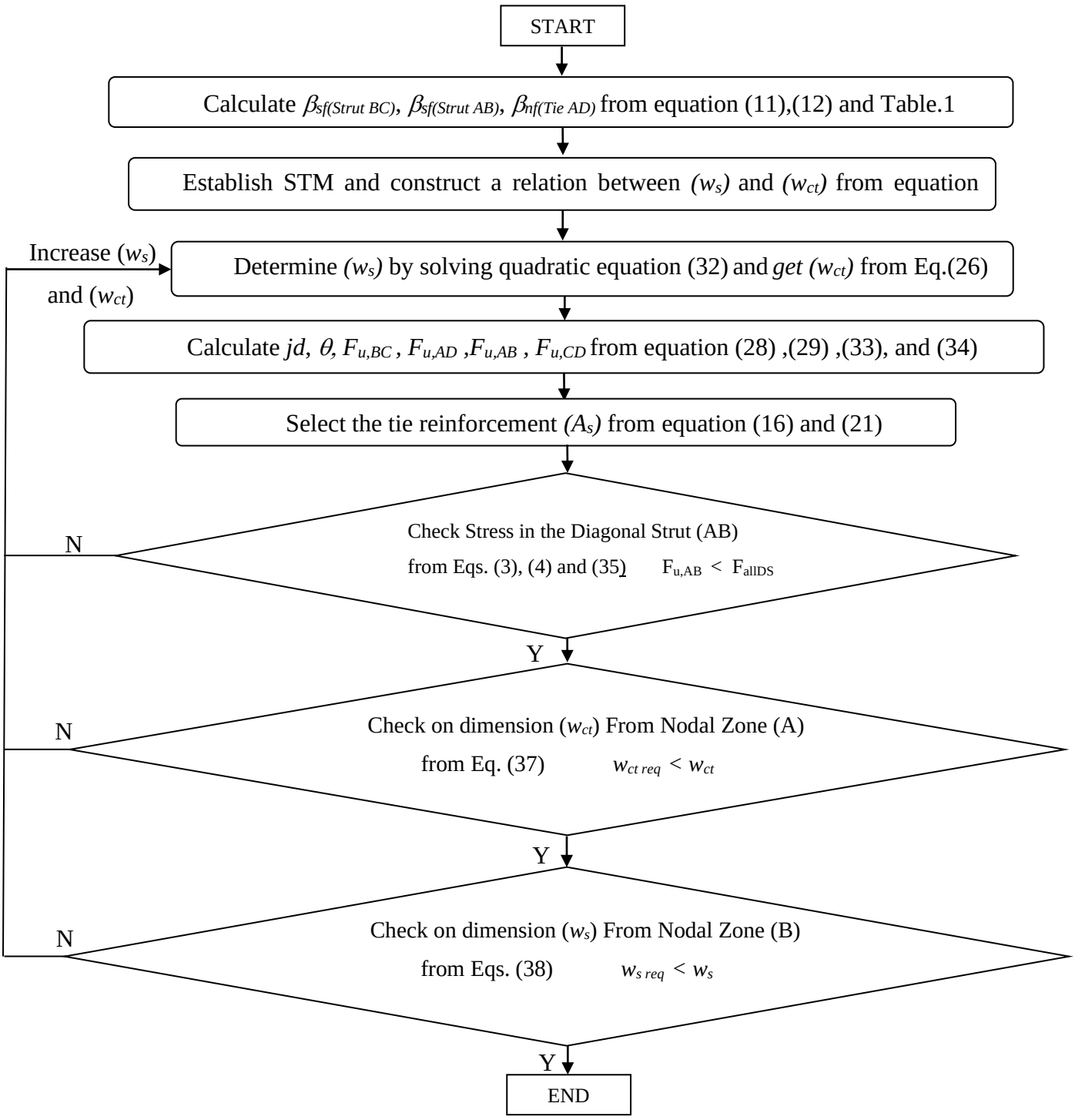


Fig. 6. Flow Chart for Design of HSFRC Deep Beams.

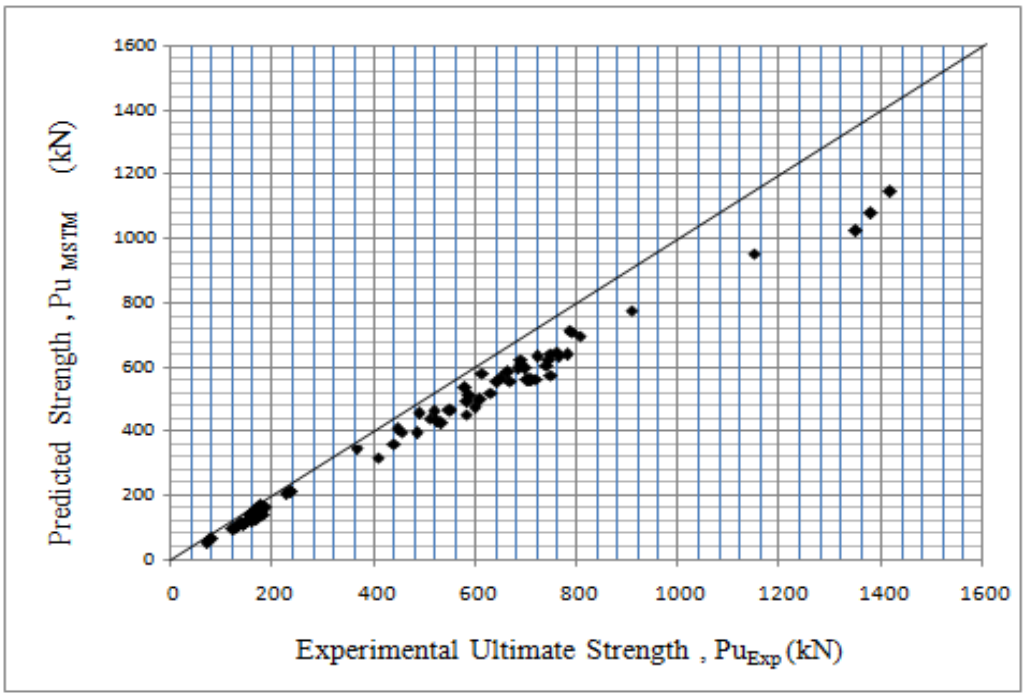


Fig.7. UltimateStrength Predications by the Modified MSTM for HSSFRC Deep Beams.

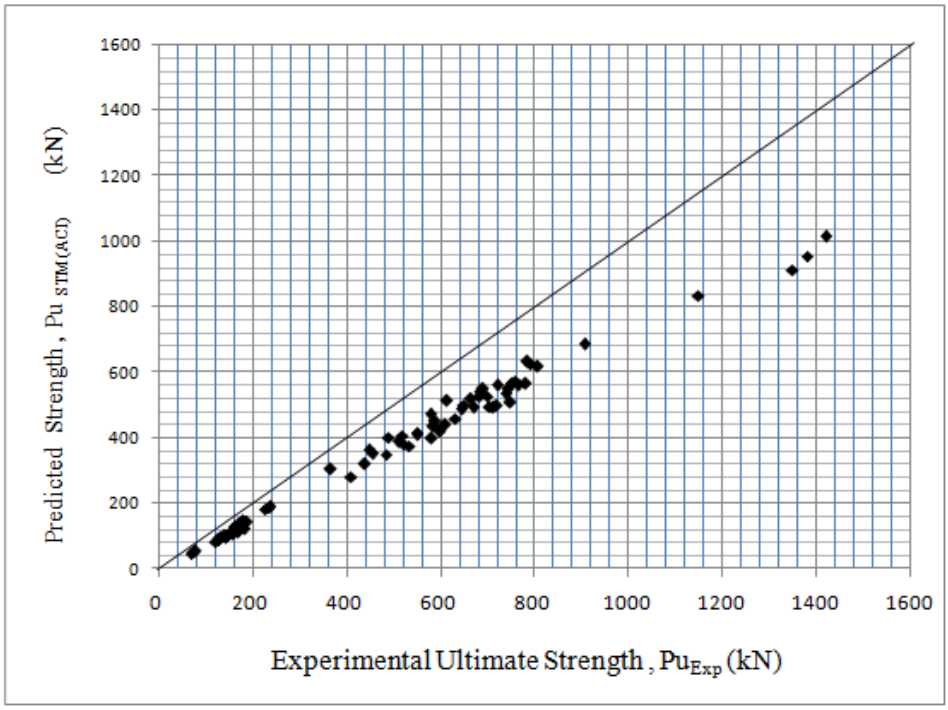


Fig.8. Ultimate Strength Predications by the STM of ACI Code 318-19 for HSSFRC Deep Beams.

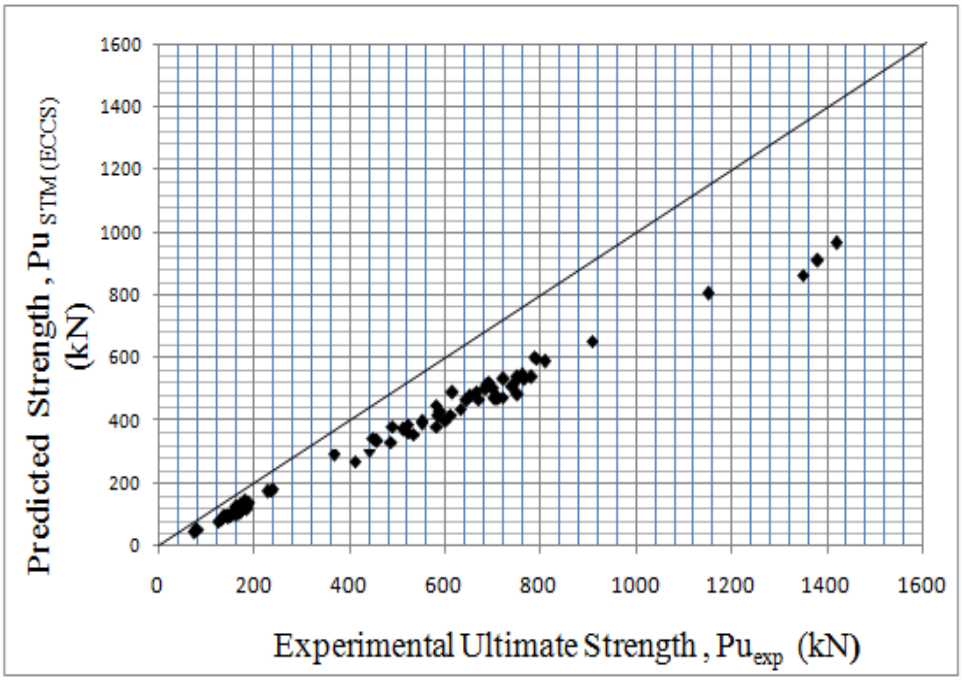


Fig.9. Ultimate Strength Predications of STM According to ECP 203-2018 for HSSFRC Deep Beams.

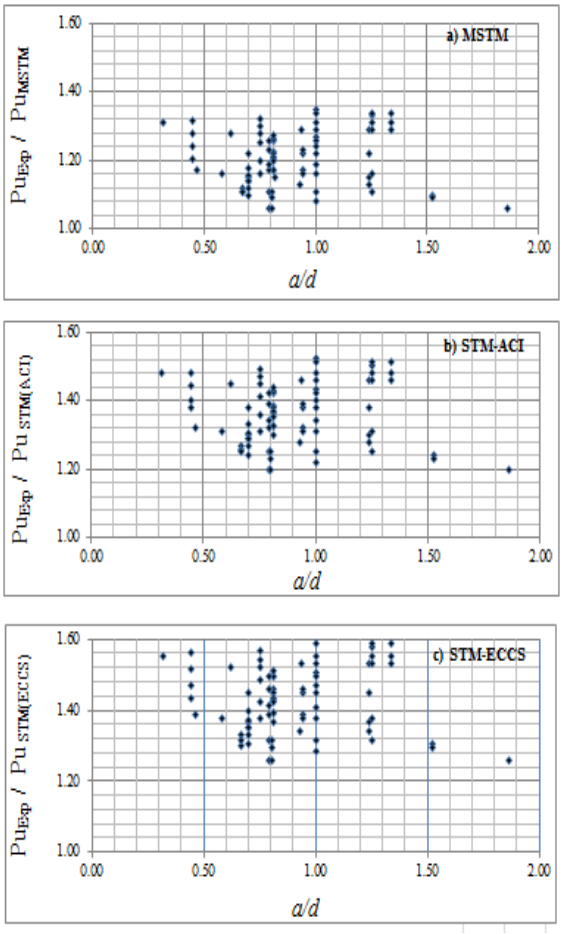


Fig.10. Effect of (*a/d*) on Ultimate Strength PredicationsDue to a) MSTM b) STM-ACI and c) STM-ECP.

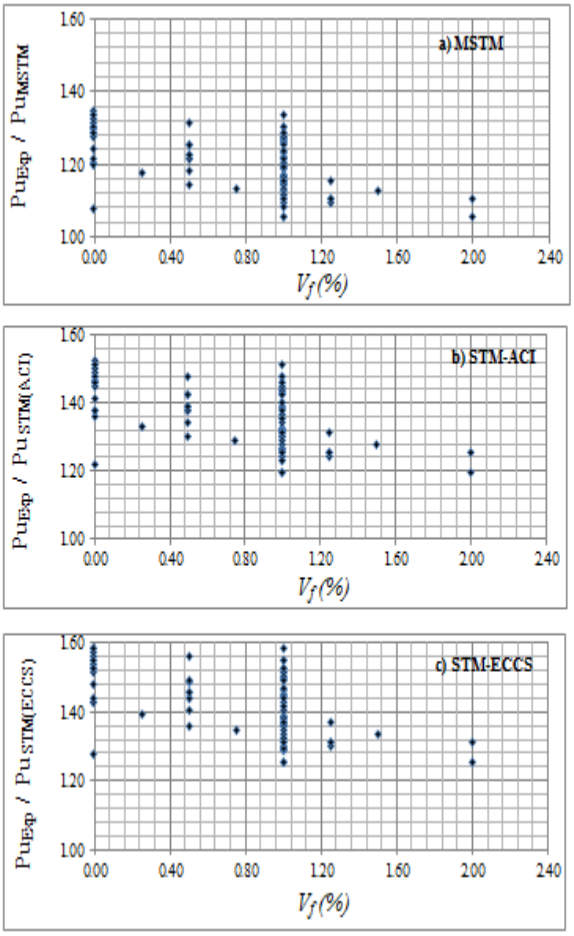


Fig.11. Effect of ($V_f$ %) on Ultimate Strength PredicationsDue to a) MSTM b) STM-ACI and c) STM-ECP.

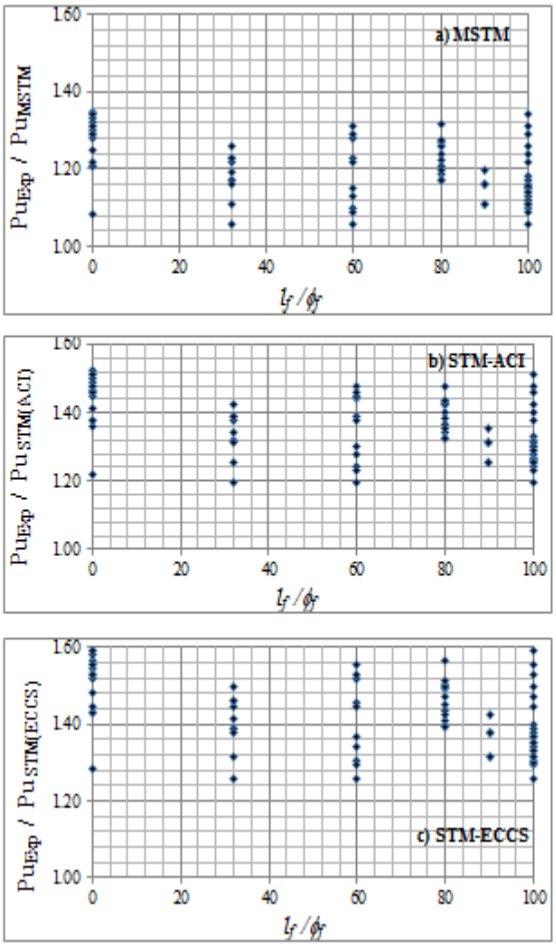


Fig.12. Effect of ($l_f$ / $\phi_f$) on Ultimate Strength PredicationsDue to a) MSTM b) STM-ACI and c) STM-ECP.

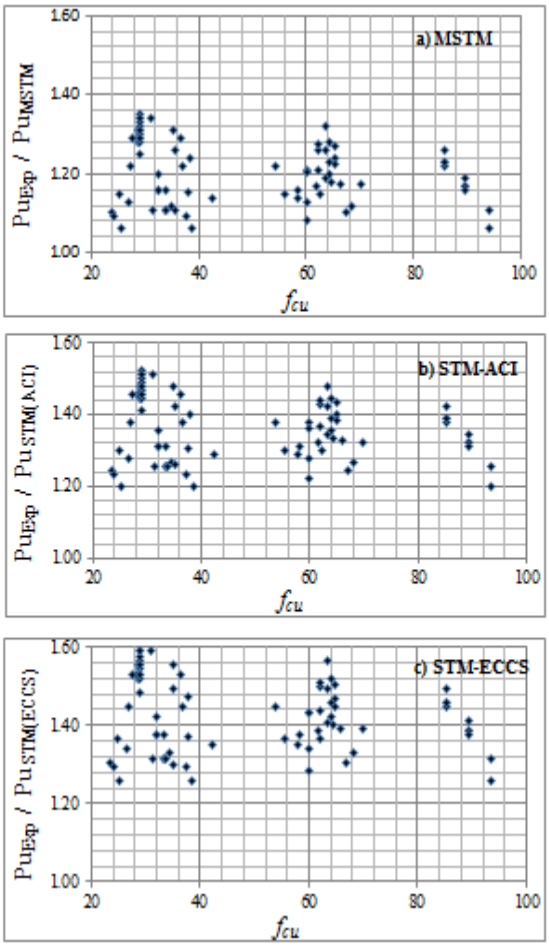


Fig.13. Effect of ($f_{cu}$) on Ultimate Strength PredicationsDue to a) MSTM b) STM-ACI and c) STM-ECP.

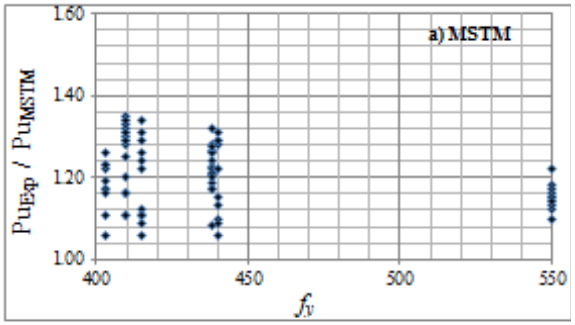


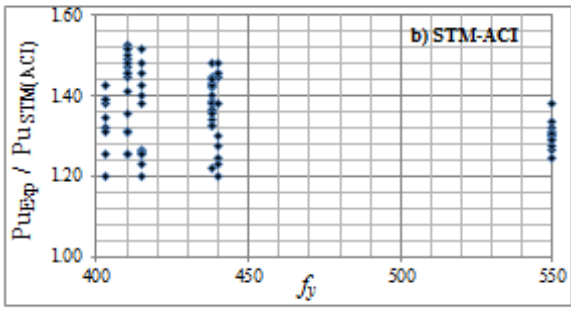


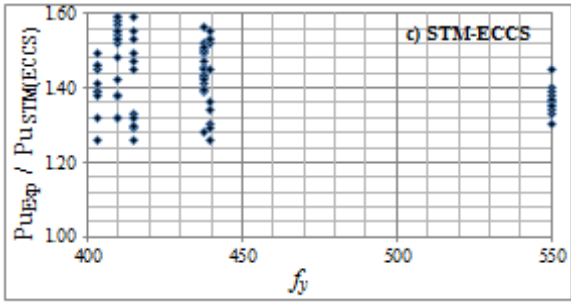


Fig.14. Effect of ($f_y$) on Ultimate Strength PredicationsDue to a) MSTM b) STM-ACI and c) STM-ECP.

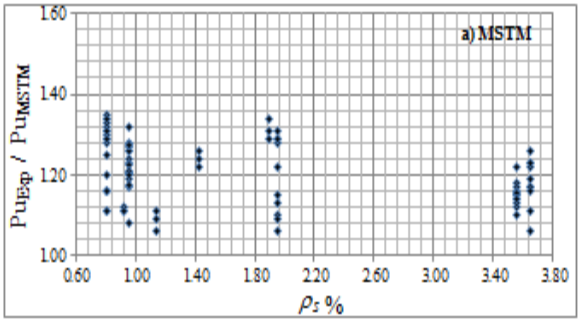


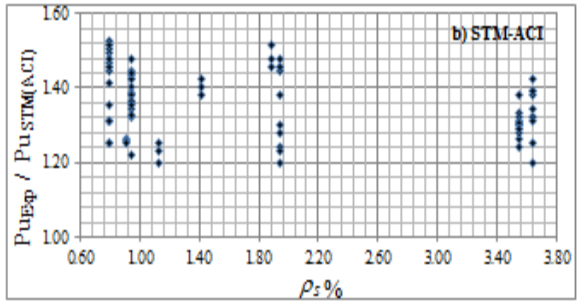


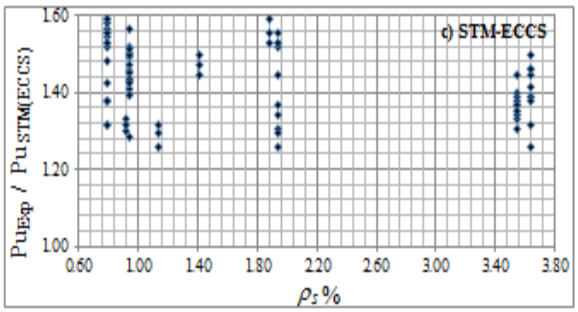


Fig.15. Effect of ($\rho_s$) on Ultimate Strength PredicationsDue to a) MSTM b) STM-ACI and c) STM-ECP.

## REFERENCES


[1] ACI Committee 318. ACI 318R-19. Building code requirements for structural concrete (ACI 318-11) and commentary (ACI 318R-19). Farmington Hills, Mich., USA: American Concrete Institute (ACI); 2019.

[2] Demeke, A., and Tegos, I. A., Steel fiber reinforced concrete in biaxial stress tension-compression conditions. ACI Structure Journal 1994, 91(5): 579- 584.

[3] ECP 203. Egyptian code of practice for design and construction of reinforced concrete structures. Housing and Building Research Center, Ministry of Building and Construction. Giza, Egypt; 2018.

[4] El-Barbary, A. A., Performance of steel fibers reinforced concrete deep beams ,Ph.D. Dissertation, Faculty of Engineering, Shoubra, Benha University, Cairo, Egypt; 2015.

[5] Foster, S. J., and Malik, A. R., Evaluation of efficiency factor models used in strut-and-tie modeling of non-flexural members. ASCE Journal Structure Engineering 2002; 128(5): 569–577.

[6] Giuseppe, C., Flexural behavior of steel fibrous reinforced concrete deep beams. ASCE Journal Structure Engineering 2012; 138(2): 235-246.

[7] Hasan, A.Q. , Structural behavior of concrete flange continuous deep beams with carbon fiber reinforced polymer (CFRP). Civil and Environmental Research, Vol.10, No.7,pp. 11-16, 2018.

[8] Zakaria, M. Salah, D. Mahmoud, M. and Awadallah, Z.,Enhancement the shear behavior of concrete beams reinforced with hybrid-wires bars by using steel fibers. Journal of Advanced Engineering Trends, Vol. 41, no. 1, pp. 55–70, 2022.

[9] Beshara , F.B.A. Shaaban, I.G. and Mustafa, T.S. , Strut-and-tie modeling of R.C. continuous deep beams. 13th Arab Structural Engineering Conference University of Blida, December, 2015 Algeria

[10] Sandeep M.S., Nagarajana,P. , Shashikalab, A.P. and Habeebc ,S.A., determination of strut efficiency factor for concrete deep beams with and without fiber, Advances in Computational Design, Vol. 1, no. 3, pp. 253-264,2016.

[11] Jalil, A.M. Hamood, M. J. Abdul-Razzaq, K. S., and Mohammed, A. H. , Applying different decentralized loadings on RC continuous deep beams using STM. International Journal of Civil Engineering Technology., Vol. 9, no. 11, pp. 2752–2769, 2018.

[12] Mohammedali, T.K. and Jalil,A.M., STM experimental verification for reinforced concrete continuous deep beams. International Journal of Civil Engineering and Technology (IJCIET) Vol. 10, Issue 2, pp.2227–2239, 2019,

[13] Singh , S.K. , Kaushik, K.F. Naveen,M. and Sharmab,S., Design of a continuous deep beam using the strut and tie method , Asian Journal of Civil Engineering ,Building and Housing ,Vol. 7, no. 5, pp. 461-477 ,2019.

[14] Mansur, M. A., and Ong, K. C. G., Behavior of reinforced fiber concrete deep beams in shear. ACI Structure Journal 1991; 88(1): 98-105.

[15] Mustafa, T.S., Behavior of high strength fiber reinforced concrete beams, MS.C.. Dissertation, Faculty of Engineering, Shoubra, Benha University, Cairo, Egypt; 2007.

[16] Narayanan, R., and Darwish, I. Y. S., Fiber concrete deep beams in shear. ACI Structure Journal, 1988; 85(S17): 141-149.

[17] Patel,V. R., Mojidra, B. R., and Pandya, I. I., Ultimate shear strength of fibrous moderate deep beams without stirrups. International Journal of Engineering Research and Development, (IJERD); 2012;1(1):16-21.

[18] Kumar G. R. and Singh S.P., Steel fibers as replacement of web reinforcement for RCC deep beams in shear. Asian Journal of Civil Engineering 2007; 8(5): 479-489.

[19] Yousef, A. M., Shear strength prediction of high- strength fiber reinforced concrete deep beams. 10th International Colloquium on Structural and Geotechnical Engineering; 2003; Ain Shams University, Cairo, Egypt: 1-19.